Sea level changes mechanisms in the MPI-ESM under FAFMIP forcing conditions

Xiaolin Zhang[1,3] · Sayantani Ojha[1,4] · Armin Köhl[1] · Helmuth Haak[2] · Johann H. Jungclaus[2] · Detlef Stammer[1]

© The Author(s) 2022

Abstract

Mechanistic causes for sea level (SL) change patterns are analyzed as they emerge from the Coupled Model Intercomparison Project Phase 6 (CMIP6) endorsed Flux-Anomaly-Forced Model Intercomparison Project (FAFMIP) coupled climate experiments imposing individual forcing anomalies in wind stress, heatflux and freshwater flux to the Max-Planck-Institute Earth System Model (MPI-ESM). It appears that the heat flux perturbations have the largest effect on the sea level. In contrast, the direct impact of momentum and freshwater flux anomalies on SL anomalies appear to be limited to some region e.g. the Southern Ocean, Arctic Ocean and to some extent the North Pacific and North Atlantic Ocean. We find that thermosteric changes dominate the total SL change over large parts of the global ocean, except north of 60 °N where halosteric changes prevail. An analysis of added and redistributed components of heat and freshwater further suggests that the added component dominates the thermosteric SL and the redistributed component dominates the halosteric SL. Due to feedback processes a superposition of all forcing components together leads to the simulated sea level changes in each individual experiment. As a result, large surface heat flux anomalies over the Atlantic lead to wind stress change outside of the Atlantic through teleconnections, which in turn appear to be the primary driving agent for changes of sea level outside of the Atlantic in all three experiments. The associated wind driven Sverdrup stream function implicates that outside of the Atlantic most of the feedback can be explained by changes in the Sverdrup circulation.

Keywords Climate change · Sea level · Ocean dynamic · Climate modeling

1 Introduction

Regional sea level rise is an inescapable consequence of climate change that can directly impact coastal societies with far reaching consequences for their safety and their economy. Contributions to regional sea level change originating from the solid earth in response to a terrestrial ice mass loss can be significant and, in few places, actually dominate the sea level response to anthropogenic forcing. However, over many parts of the world, regional sea level rise is dynamic and results primarily from the response of the ocean circulation to climate-change related forcing variations.

The main drivers for dynamic regional sea level changes are fluctuations in the atmospheric forcing, notably wind stress fields, and surface heat and freshwater fluxes between the atmosphere and the ocean. The associated adjustment of the ocean circulation can lead to broad-band sea level variability on various time scales (Stammer et al. 2013); of interest for decision makers are especially regional secular sea level change pattern (trends), which are pronounced in centennial climate projections (Slangen et al. 2014). Together with contributions from the solid earth response to regional sea level change, they can lead to significant deviations of coastal sea level from a global mean around the globe (Carson et al. 2016). However, some—yet to be quantified—fractions of the longer-term changes can also result from internal variability of the system on decadal to centennial time scales (Carson et al. 2015).

✉ Armin Köhl
  armin.koehl@uni-hamburg.de

1   Institut für Meereskunde, Universität Hamburg, CEN, Hamburg, Germany

2   Max Planck Institute for Meteorology, Hamburg, Germany

3   Present Address: Department of Earth and Planetary Sciences, Kyushu University, Fukuoka, Japan

4   Present Address: Earth and Space Sciences, Indian Institute of Space and Technology, Thiruvananthapuram, Kerala, India

Improving anthropogenic sea level projections and their impacts require an improved understanding of mechanistic causes underlying coastal sea level projections. The Flux-Anomaly-Forced Model Intercomparison Project (FAFMIP) Experiment was proposed and implemented as part of the Coupled Model Intercomparison Project Phase 6 (CMIP6) (Gregory et al. 2016) to rationalize differences occurring between the projections of individual models (e.g., see Slangen et al. 2014). It was designed to identify forcing mechanisms of regional sea level response such as changes in the ocean density and circulation pattern, under well-defined conditions. Imposed forcing anomaly patterns for wind stress, heat, and freshwater fluxes were derived from CMIP5 "1pctCO2" runs at the time when doubled CO_2 concentration has been reached. Gregory et al. (2016) provide more details on FAFMIP and first results in terms of ensemble mean and spread of the total resulting sea level anomalies and the comparison to those resulting from individual forcing using low-resolution models. More recently, Couldrey et al. (2021)showed that surface heat flux changes drive most of the sea level change pattern in the FAFMIP runs and that the spread between underlying Atmosphere–Ocean General Circulation Models (AOGCM) is caused largely by differences in their regional transport adjustment, which redistributes regional heat content differences that existed in the ocean prior to perturbation. However, the quantification of the mechanisms behind the simulated responses as a function of surface forcing agent remains unclear in previous publications.

The objective of the present paper is to quantify the response of dynamic sea level due to individual forcing changes, namely wind-stress, fresh water flux and heat flux under the idealized FAFMIP forcing and to explore the dynamic processes underlying anthropogenic trends. The study is based on the output of the Max-Planck-Institute Earth System Model (MPI-ESM) coupled AOGCM run in a high-resolution setting with individual FAFMIP forcing anomalies imposed. Our specific focus is directed at quantifying the detailed impact of change in wind stress, heat flux and freshwater flux on projected sea level change in each of those MPI-ESM runs so as to better understand underlying causes and their effect on the ocean circulation leading to the simulated sea level anomaly pattern. Novel aspects of this study include (i) the analysis of an additional passive salt experiment (see Sect. 2.2), (ii) the quantification of the impact of feedbacks between individual forcing components on the solution and (iii) focusing on the highest resolution model in the ensemble previously analyzed by Couldrey et al. (2021).

The paper is organized as follows. A description of the model and experiments are provided in Sect. 2. Section 3 summarizes the sea level response to FAFMIP forcing based on each individual experiment except wind stress. Wind stress forcing is specifically addressed in Sect. 4 discussing mechanisms behind the sea level response, including the induced forcing due to the feedback mechanisms and the impact of wind changes as an important mechanism for sea level change for all imposed forcing anomalies. Concluding remarks are provided in Sect. 5.

2 Model and experiments

2.1 Model

Our analysis is based on output of the MPI-ESM-HR version with high spatial resolution as part of the FAFMIP. High resolution refers to a horizontal resolution of close to 100 km in the atmosphere (ECHAM6.3 T127L95) and 40 km in the ocean (MPIOM1.6 TP04/L40). The design and performance of MPI-ESM1.2-HR is documented in Müller et al. (2018) and Mauritsen et al. (2019). The runs were performed as part of the CMIP6 FAFMIP experiment during which the model is forced with momentum, heat and freshwater flux anomalies inferred at doubled CO_2 concentration from the ensemble mean of the CMIP5-1pctCO$_2$ experiments, in which CO_2 increases by 1% per year. All experiments started from the piControl experiment and ran over 70 years. The average of the last ten years relative to the control run is used in the following to represent the long-term change of the sea level under various forcing changes. Accordingly, all changes marked as Δ below are understood as changes estimated as the difference of fields from the forced experiment relative to the control, both averaged over the final decade of the 70 years.

2.2 Experiments

As described in Gregory et al. (2016), FAFMIP consists of three tier-1 experiments, notably FAF-stress, FAF-heat and FAF-water, imposing perturbations in momentum, heat and freshwater fluxes respectively. All surface forcing perturbations are applied at the ocean surface, such that sea ice is not directly affected (Fig. 1, see also Couldrey et al. 2021). However, there will be indirect effects on sea ice due to the changes of heat and freshwater in response to all the perturbations. The respective perturbations to the air-sea fluxes of heat, water, and momentum are applied in five different experiments as listed in Table 1.

In FAF-heat, the heat flux perturbation is applied as a forcing to the Sea Surface Temperature (SST). The perturbation is strongly positive in the North Atlantic and in the Southern Ocean. However, the forcing is applied only to the ocean temperature that is not "seen" by the atmosphere. This is done because, in case the SST was forced with a heat flux perturbation, changes in SST would lead to an
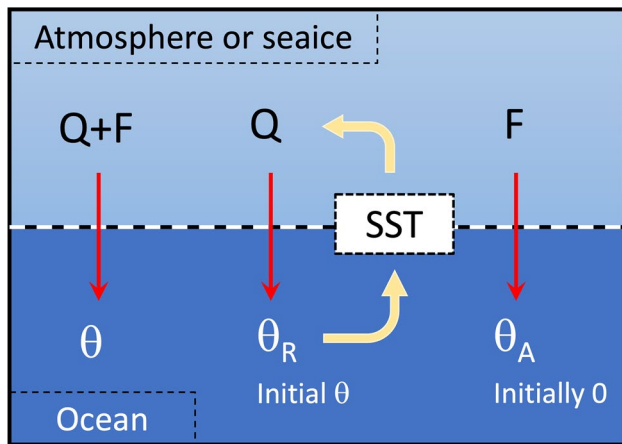
Fig. 1 Description how the flux perturbation in FAF-heat and FAF-all affects various tracers, redrawn from Gregory et al. (2016). Q is the net surface heat from the atmosphere and sea ice into the ocean and F is the flux perturbation. The SST based on the redistributed temperature tracer θr (independent of F) is used to calculate the surface heat flux to atmosphere and sea ice

opposing air–sea flux. This flux would reduce the perturbation and heat the atmosphere indirectly, which would provide response in the other forcing components. To avoid this, a redistributed temperature tracer, θr is introduced, which is initialized to equal the temperature field of the model and is exchanged around the ocean using the same circulation schemes as θ, except that it is not forced by the surface heat flux perturbation (Fig. 1). Because θr is not affected by the perturbation flux, fields of θr and θ quickly diverge from each other by a value equal to a "passive temperature", θp (see below).

The atmosphere is decoupled from the SST of θ, and instead only sees the surface field of θr. As a result, the perturbation gets added to the ocean, where it accumulates and modifies seawater density, and changes the ocean circulation. The atmosphere, however, does not absorb any of the added heat and is only modified by changes to surface θr that arise indirectly through the changing ocean circulation. In contrast, the heat flux perturbation is applied in FAF-passiveheat to a 'passive temperature' tracer, θp. FAF-passiveheat thus functions as a control, since its climate is not forced and experiences only internal variability. This

experiment's climate is the same as an unperturbed piControl simulation, except the extra tracer allows for the passive uptake of the heat perturbation to be quantified. θp is initially set to 0 everywhere, and forced at the surface. The tracer moves through the ocean via the same scheme that the model uses, to advect and diffuse temperature, θ, without altering the circulation. Since the perturbation has positive and negative values locally, θp can be positive and negative.

The ocean freshwater flux perturbation applied to the ocean in FAF-water has a very small global annual mean and principally only redistributes freshwater. The perturbation thereby intensifies evaporation in the mid latitudes, and intensifies precipitation elsewhere: notably the equatorial Pacific, the Southern Ocean, the Arctic Ocean, and the high latitude North Pacific and North Atlantic. There is no perturbation applied over land and thus river discharge is not altered. To quantify the impact of the circulation changes on the redistribution of salinity a redistributed salinity tracer, Sr, is added to the FAF-water experiment, which similar to the redistributed temperature tracer, is not forced by the perturbation fluxes but feels only atmospheric fluxes. The passive salt experiment is unique in that it is not part of the "official" FAFMIP protocol.

Similar to the FAF-passiveheat experiment, the additional experiment, FAF-passivesalt, applies the water flux perturbation to the 'passive salinity' tracer, Sp. FAF-passivesalt can also function as a control, since its climate is not forced at all, and all experienced variability is of internal nature. This experiment's climate therefore is the same as that of an unperturbed piControl (reference) simulation, except the extra tracer allows for the passive uptake of the water perturbation to be quantified. Sp is initially set to 0 everywhere, and forced additionally at the surface with the perturbation. The respective tracer moves through the ocean via the same mechanisms that advect and diffuse salinity, S, but without altering the circulation. Since the perturbation has positive and negative values locally, Sp can be positive and negative.

The surface momentum perturbation applied in FAF-stress is mainly characterized by an intensification of the Southern Ocean westerlies. The perturbation has smaller effects on the zonal and meridional downward momentum fluxes in the mid latitudes. The perturbation is added to the momentum

Table 1 Flux-anomaly-forced model intercomparison project (FAFMIP) experiments

Experiment	Name	Ocean surface flux perturbation
1	FAF-all	All from FAF-stress, FAF-heat and FAF-water
2	FAF-stress	Zonal and meridional wind stress
3	FAF-heat	Heatflux
4	FAF-water	Freshwater flux
5	FAF-passiveheat	Heat as in FAF-heat, but forcing a passive tracer
6	FAF-passivesalt	Freshwater as in FAF-water, but forcing a passive tracer

balance of the ocean surface, such that it does not directly affect schemes that depend on wind stress or ice stress.

All three perturbations are applied together in the FAF-all experiment. This experiment serves two purposes: to assess how well the perturbations mimic the effect of CO_2 forcing as in 1pctCO2, and to determine the extent to which the perturbations nullify or amplify each other's effects on sea level when applied simultaneously. If the flux perturbations interact with each other when applied together in FAF-all, then the FAF-all sea level response will not equal the sum of the sea level responses to the individual perturbations.

2.3 Sea level changes

Any dynamic sea level change, $\Delta\zeta$, can be separated into the two components (see also Gill and Niiler 1973):

$$\Delta\zeta = \Delta\zeta_N + \Delta\zeta_{ST}, \tag{1}$$

where $\Delta\zeta_{ST}$ represents the steric change, while $\Delta\zeta_N$ is the part of dynamic sea level change that is concerned with changes in the bottom pressure. The steric contribution to dynamic sea level change can be split into thermosteric ($\Delta\zeta_T$) and halosteric ($\Delta\zeta_S$) components

$$\Delta\zeta_{ST} = \Delta\zeta_T + \Delta\zeta_S, \tag{2}$$

which can be estimated from temperature and salinity fields according to

$$\Delta\zeta_T = \int_{-H}^{\zeta} \alpha\Delta T dz \tag{3}$$

$$\Delta\zeta_S = -\int_{-H}^{\zeta} \beta\Delta S dz \tag{4}$$

Here the thermosteric sea level change, $\Delta\zeta_T$, is the depth integral (from the full ocean depth, H to the surface, ζ) of the change in temperature (ΔT, in °C) multiplied by the pressure p dependent seawater thermal expansion coefficient, $\alpha(T,S,p)$. Similarly, the halosteric component can be estimated by using the change in salinity (ΔS) and the haline contraction coefficient of seawater, $\beta(T,S,p)$. In each grid box, α and β were calculated using the local temperature, salinity and pressure fields of each simulation of the final decade based on the standard nonlinear equations of state.

For each steric component, the SL can be separated into contributions resulting from locally added, as well as redistributed heat and freshwater contents and nonlinear contributions considering correlations between added heat or freshwater and circulation changes as summarized in Fig. 2 (also see discussions provided in Couldrey et al. 2021):

- The added thermosteric and halosteric components are estimated from the added temperature θp and added salinity Sp, respectively.
- The redistributed thermosteric component is estimated from the redistributed temperature of FAF-heat and from the regular temperature of FAF-water and FAF-stress, respectively.
- The redistributed halosteric component is estimated from the redistributed salinity of FAF-water and from the regular salinity of FAF-heat and FAF-stress, respectively.
- The nonlinear thermosteric component then follows as a residual, i.e. the difference of the thermosteric signal of FAF-heat minus the sum of the added and redistributed

Fig. 2 Schematic of the decomposition of the sea level response. For the decomposition into contributions from different FAFMIP experiments it is assumed that the total SL from FAF-all can be represented by the sum of the individual forcing experiment, which turned out to hold quite well
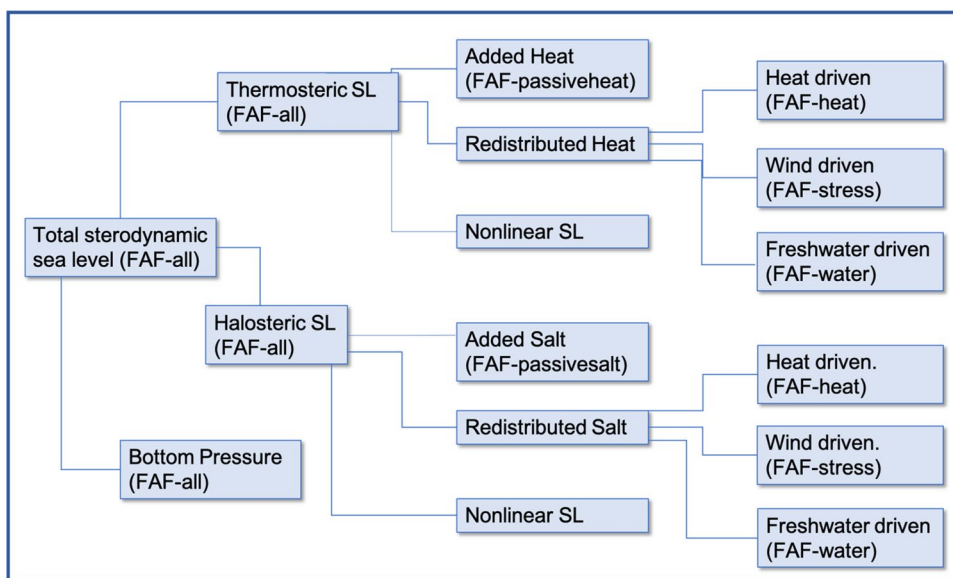
thermosteric signals of FAF-passiveheat and FAF-heat, respectively.

- The nonlinear halosteric component is the difference of the halosteric signal of FAF-water minus the sum of the added and redistributed halosteric signals of FAF-passivesalt and FAF-water, respectively. The nonlinear component describes how changes of the ocean transport redistribute the added salinity.

Our overarching goal is to explain the regional sea level response in the 1% CO_2 scenario for which FAFMIP attempts to decompose contributions resulting from different forcing perturbations. Figure 2 illustrates how the decomposition of FAF-all into thermosteric, halosteric and bottom pressure components is further decomposed into added, redistributed and nonlinear response terms, and how these relate to contributions from different forcing perturbations (wind stress, heat and fresh water). For the decomposition of the redistributed component, we identify the thermosteric responses from the experiments with added wind and freshwater perturbations and the halosteric responses from the experiments with added wind and heatflux perturbations, as their respective added heat or added freshwater is zero.

Significance is tested on the differences to the control run assuming that both runs are uncertain causing the expected variance of the difference (the null hypothesis) to be twice the variance as estimated from the 10-year means of the 500 year-long control run. Although sea level change signals are shown including the global mean thermosteric signal, significance tests were performed on the signals without the global mean signals. Therefore, the pronounced negative dynamic sea level change in the Southern Ocean remains significant, while including the global mean would yield values near zero there, causing the most pronounced signal of regional sea level change to remain largely insignificant.

3 Sea level response to FAFMIP forcing

3.1 Thermosteric versus halosteric and mass-related changes

To set the stage, we examine first SL response, defined as combination of the global mean thermosteric with dynamic sea level, to all forcing perturbations and compare this with the 1pctCO2 scenario from which the forcing perturbations were generated. Note, forcing perturbations have originated from the CMIP5 ensemble mean, while here we compare to the particular response in the MPI-ESM-HR 1pctCO2 experiment (Fig. 3a, b).

Shown in Fig. 3b is the $\Delta\zeta$ field as it results from the FAF-all experiment averaged over the last decade of the 70 year-long experiment relative to passive-heat, which follows the evolution of the control. The respective field is positive everywhere except in a few places of the Southern Ocean and the northwestern Pacific Ocean. The largest rise of about 50 cm resides in the North Atlantic Ocean. In the Southern Ocean and northwestern Pacific Ocean, a fall of about 10 cm can be observed. In comparison to SL based on the 1pctCO2 experiment (Fig. 3a), these amplitudes are of similar pattern, but in most regions nearly twice of the 1pctCO2 amplitude they are intended to represent. Garuba and Klinger (2016) describe this enhancement as redistribution effect related to the reduction of the Atlantic meridional overturning circulation (AMOC) and the associated cooling in the North Atlantic. The AMOC weakening was found to be 10% stronger in coupled models in comparison to uncoupled ocean models (Todd et al. 2020). They also explain that the changes in differential heating reduces the AMOC and that the changes in atmosphere minus ocean temperature gradient enhances the coupled response. In comparison to Couldrey et al. (2021, their Fig. 3) the fields shown in Fig. 3a, b look similar, taking into account that a global mean thermosteric component is present only in our figures. And because we show results from only one model and one ensemble member, our results show finer structures. Nevertheless, largescale structures compare well.

To justify the decomposition into contributions from different forcing components, linear superposition of the responses is assumed to be valid. In Fig. 3b, c we evaluate this assumption by comparing the sum of the sea level responses to individual forcing components to their joint action in FAF-all. Despite the sum of the responses appears to be larger almost everywhere, the differences (Fig. 3d) show low significance. The reason for the low significance of the considerable differences is the large impact the climate variability on the composites. Note that the response of the sum involves six elements, with three of them are identical, which renders its variance 12 times larger than that of the control. Nevertheless, the consistently larger response of the sum points to non-linear damping of large responses.

The thermosteric and halosteric contributions to the total sea level are shown in Fig. 4a, b. As in Couldrey et al. (2021), the similarity between the spatial pattern of total SL (Fig. 3b) and the thermosteric sea level changes (Fig. 4a) suggest that the FAF-all dynamic sea level changes are primarily thermosteric in nature. We note that the thermosteric sea level change shows a dipole over the North Atlantic Ocean. However, this is not visible in the total SL change as the thermosteric sea level fall in the northeast part is being compensated by the strong halosteric sea level rise over that region. We also note that in some regions of the Atlantic, the halosteric sea level change compensates part of the thermosteric sea level change as it was noted by Pardaens et al. (2011). To some extent, the opposite holds for the tropical Pacific

Fig. 3 Projected sea level (cm) change averaged over the last decade of the 70-year period relative to the piControl run based on **a** 1pctCO2 experiment and **b** FAF-all, **c** the sum of FAF-heat, FAF-stress and FAF-water and **d** the difference between the sum in (**c**) and FAF-all. All regions outside the white stippled areas are significant at the 95% level
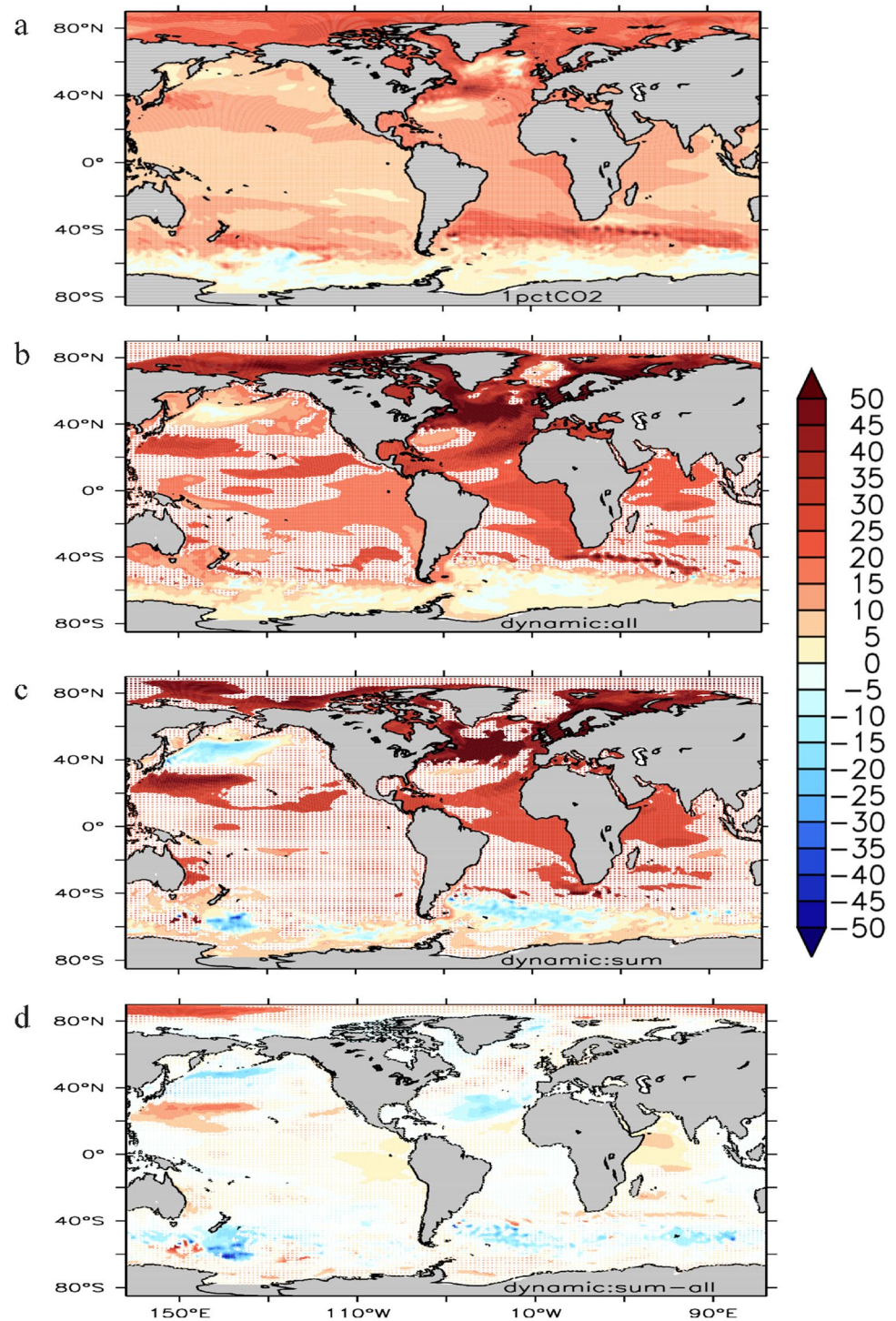
Ocean, where in the western regions halosteric changes amplify thermosteric changes. The thermosteric response is dominated by its global mean which dynamically is unimportant. If the global mean is subtracted, a fair amount of compensation between thermosteric and halosteric response is widespread. In both cases we see a clear role played by salinity changes to reduce sea level change.

The part of dynamic sea level change that is concerned with changes in the bottom pressure, $\Delta\zeta_N$, is shown in Fig. 4c. It is the residual between the thermosteric and halosteric components and the total SL. The field shows positive amplitudes over all major shelf systems caused there by regional mass gains in response to open-ocean steric sea level rise (see also Landerer et al. 2007). Most noticeable,

Fig. 4 Projected sea level (SL) change in cm as decomposition of the FAF-all SL into **a** thermosteric, **b** halosteric, and **c** bottom pressure changes. All regions outside the white stippled areas are significant at the 95% level. Bottom pressure changes are significant nearly everywhere because the pattern is the fingerprint of the highly significant global mean thermosteric sea level rise
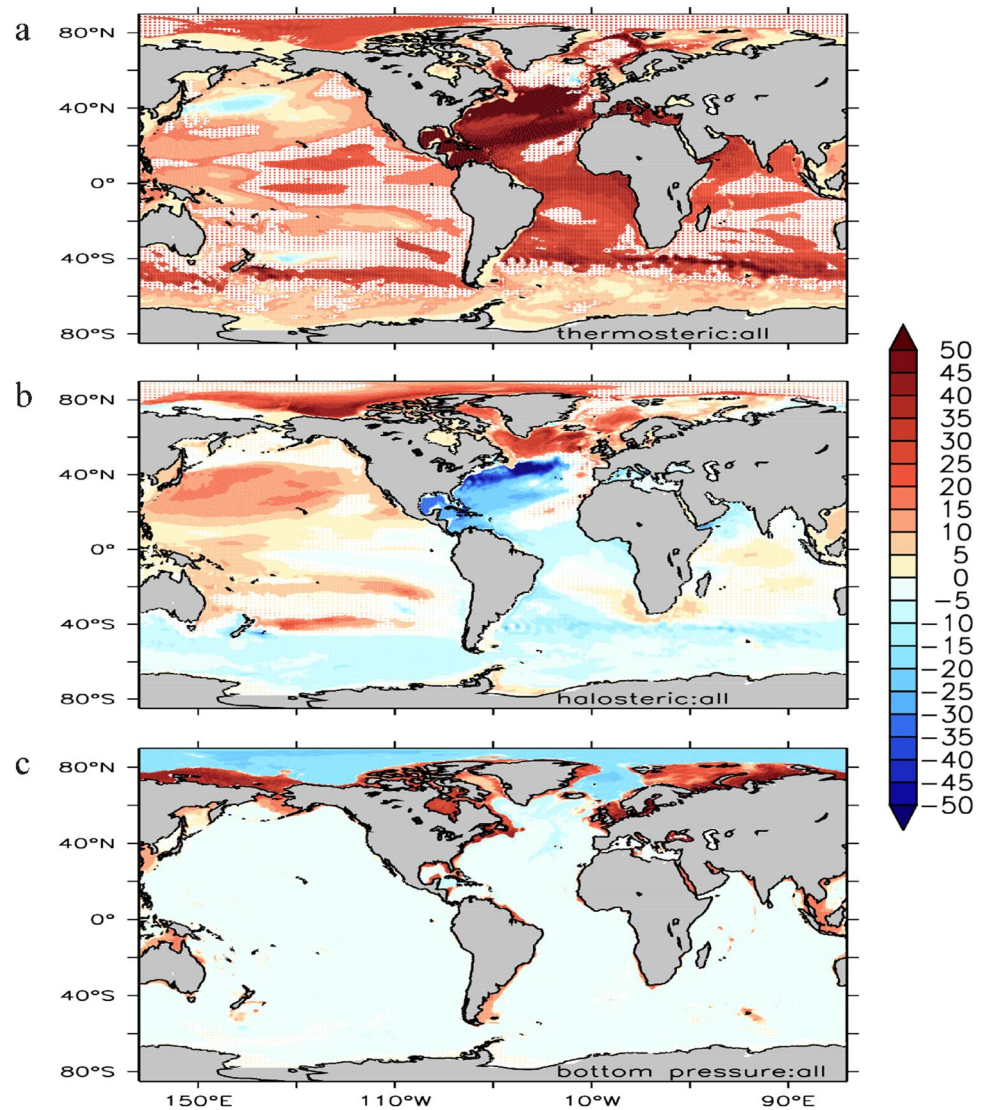
this holds along the Siberian coast where $\Delta\zeta_N$ reaches about 30 cm. To compensate the mass-conserving shelf-sea bottom pressure rise, $\Delta\zeta_N$ has to be negative elsewhere. This holds especially over the Arctic, which, although showing the largest negative signal, contributes only little more than one third of the mass. The signal over the remaining global open ocean is not as dramatic as that over the Arctic; however, it is still negative, balancing the larger part of the mass gain on the Arctic shelf and the remaining major shelf regions around the world.

Shown in Fig. 5 are the zonal averages of the total SL changes, as well as thermosteric, halosteric and bottom pressure related changes shown in Fig. 4. For total SL, the zonal mean amounts to about 25 cm between 40 °S and 50 °N, and increases to about 40 cm northward, near 60 °S it approaches zero. Consistent with Fig. 4, the total SL change over the global ocean is mostly thermosteric, while north of 60 °N contributions from the halosteric component prevail (around

30 cm); only to a lesser degree they can also be observed south of 20 °S. The bottom pressure plays an enhance role between 50 and 80 °N (about 20 cm). Further poleward amplitudes show the opposite sign (about−20 cm).

3.2 Contribution from added and redistributed heat and freshwater

With respect to the thermosteric changes emerging from FAF-heat (Fig. 6a), we can see a thermosteric SL rise almost everywhere except in the Southern Ocean as well as in the subpolar northern hemisphere, where a thermosteric SL fall can be observed. Associated with the latter, negative anomalies is a dipole pattern in the North Atlantic Ocean involving a fall in the subpolar gyre flanked by a rise along the North Atlantic Current. The North Pacific shows a similar pattern, albeit weaker in amplitude. In comparison to Fig. 3b representing FAF-all, we now find

Fig. 5 Zonal means of SL change fields shown in Figs. 3, 4 (in cm): total (dynamic) SL (black line), thermosteric (red line), halosteric (green line), and bottom pressure (blue line)
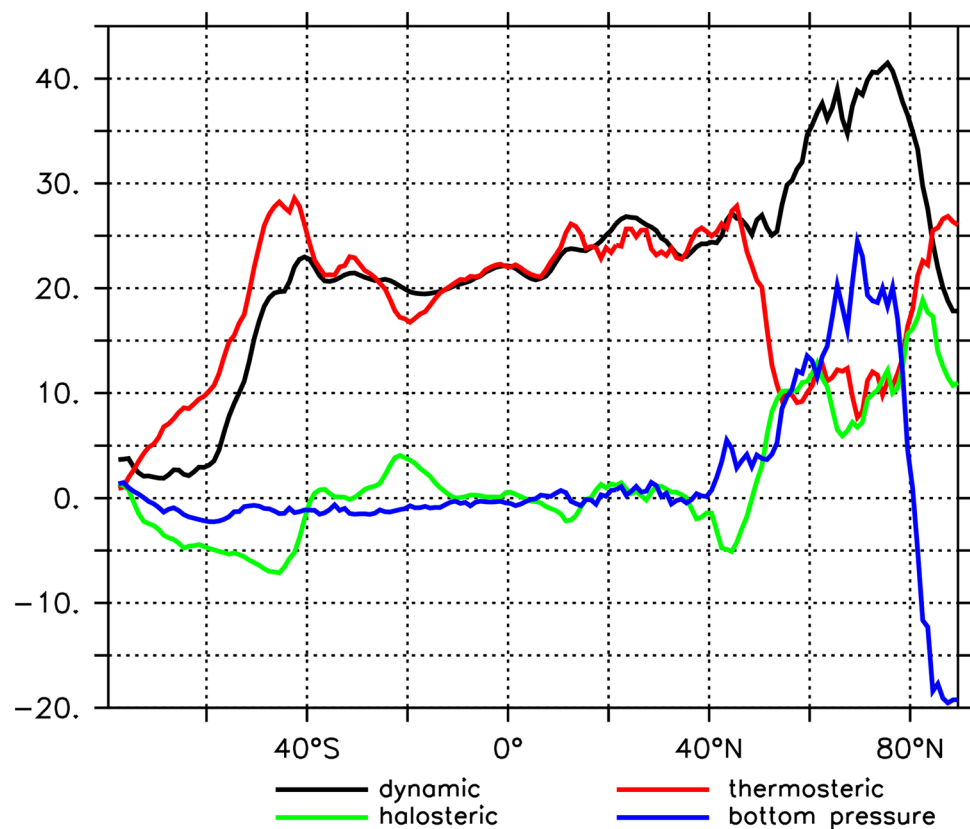
a substantially smaller amplitude in the thermosteric component in the FAF-heat experiment, suggesting that in the FAF-all experiment considerable feedbacks exist in the forcing fields that lead to a stronger heat forcing or redistribution (see below).

In comparison to the total thermosteric anomaly, the added component, shown in Fig. 5b, is larger and everywhere positive, as one would expect from the mostly positive heat flux forcing. Largest heat input appears to exist in the North Atlantic, consistent with the findings of Couldrey et al. (2021). All remaining subtropical gyres also show enhanced sea level through added heat, but weaker in amplitude.

In contrast, the sea level change due to the redistributed heat (Fig. 6c) is much more complex and shows pronounced positive and negative anomalies. Largest amplitudes reside again in the North Atlantic resulting in a negative horseshoe pattern in the subpolar and eastern subtropical basins, separated by a thin positive ridge along the North Atlantic Current advecting heat northward. Most of the other subtropical gyres also show negative patterns, whereas the tropics and the Southern Ocean exhibit positive sea level anomalies due to circulation changes. Together the added and redistributed maps reveal that in the Arctic region, the added component dominates while the redistributed component plays an opposing role. For the North Atlantic Ocean and

South Indian Ocean, the added component also dominates the sea level while the redistributed component again plays an opposing role. In contrast, in the Northern Pacific Ocean, the negative redistributed component dominates while now the added component plays an opposite role.

The nonlinear component results as the residual from the difference between total heat changes of FAF-heat to the sum of the redistributed and added heat and represent the effect that the changed circulation has on the added heat. It shows a clear negative sea level anomaly in the North Atlantic, which partially compensates the positive anomaly from the added heat (Fig. 6d). In contrast, the positive nonlinear contribution in the Arctic partially compensates the negative component resulting from the redistribution thereby substantially enhancing the sea level rise.

As discussed earlier, based on a suite of AOGCMs, Couldrey et al. (2021) also discussed the role of the added and redistributed heat in total thermosteric sea level change. The authors found that in the Indian Ocean, both the added and redistributed contributions are important, but that details are model dependent. In the North Atlantic Ocean, the added component is positive and the redistributed (non-linear) contributions are negative. In the Arctic, the redistributed, added and non-linear components are all important, with added and non-linear components are strongly positive while the

Fig. 6 **a** Total thermosteric SL change over a 70-year period relative to the piControl run from FAF-heat and its decomposition into **b** added, **c** redistributed and **d** nonlinear from calculated FAF-heat and FAF-passiveheat. See text for details. Units are cm. Regions outside the white stippled areas are significant at the 95% level. Added heat is not tested for significance since it is not expected to be affected much by climate variability and it is difficult to constitute a respective test
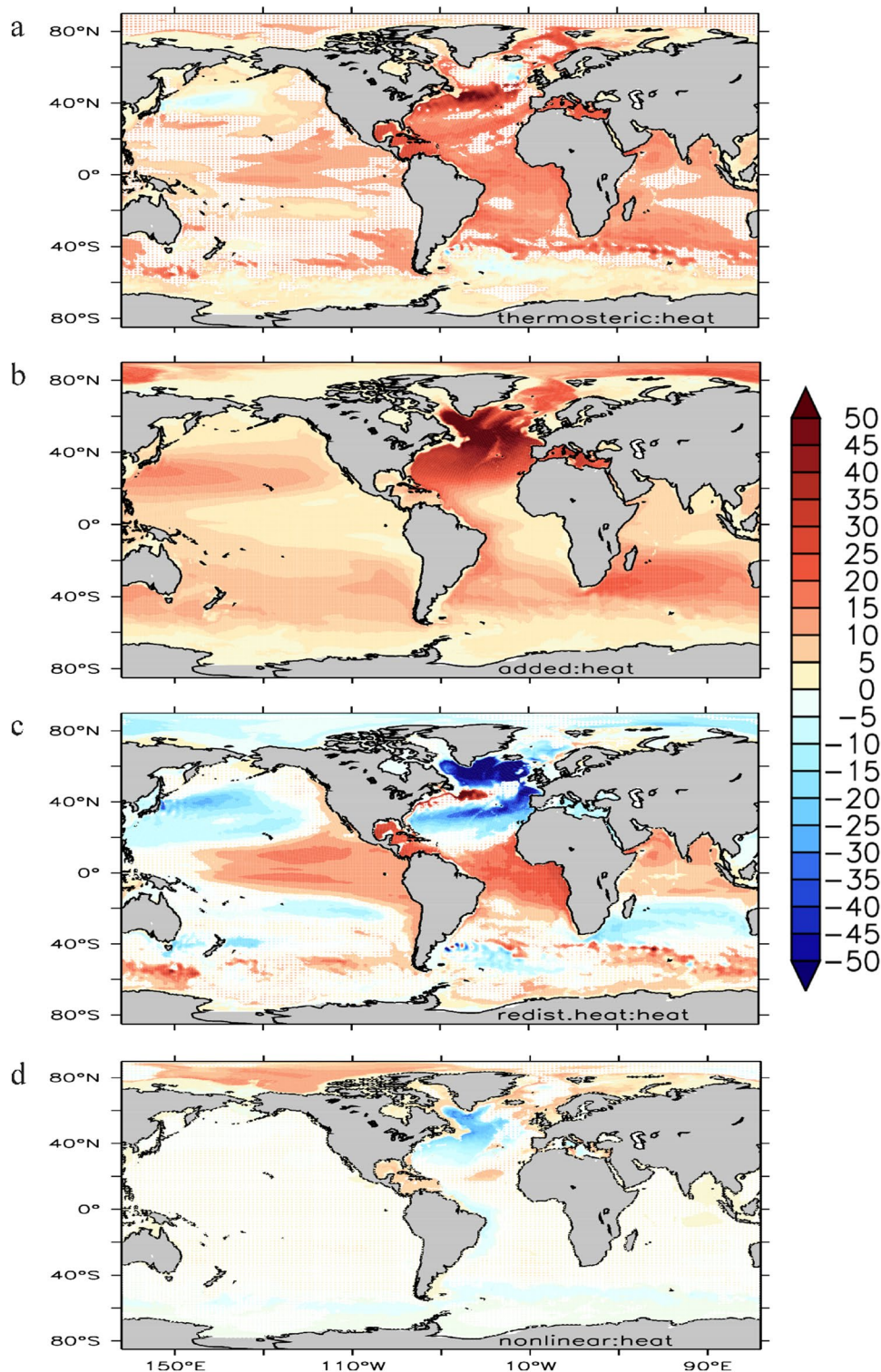
redistributed component is negative (see Figs. 6 and 12 in Couldrey et al. 2021).

For the halosteric SL resulting from FAF-water (Fig. 7), overall, the contribution to the total sea level change is smaller than the thermosteric component (about 30 cm compared to 80 cm). Moreover, anomalies are essentially balanced indicating that besides small effect resulting from the nonlinearity of the equation of state, there is no net input of freshwater into the model ocean due to FAFMIP freshwater anomalies. The total halosteric component in the FAF-water experiment (Fig. 7a) shows negative anomalies due to freshening confined essentially to the North Atlantic.

Fig. 7 As in Fig. 6, but for halosteric sea level of FAF-water and its contributions
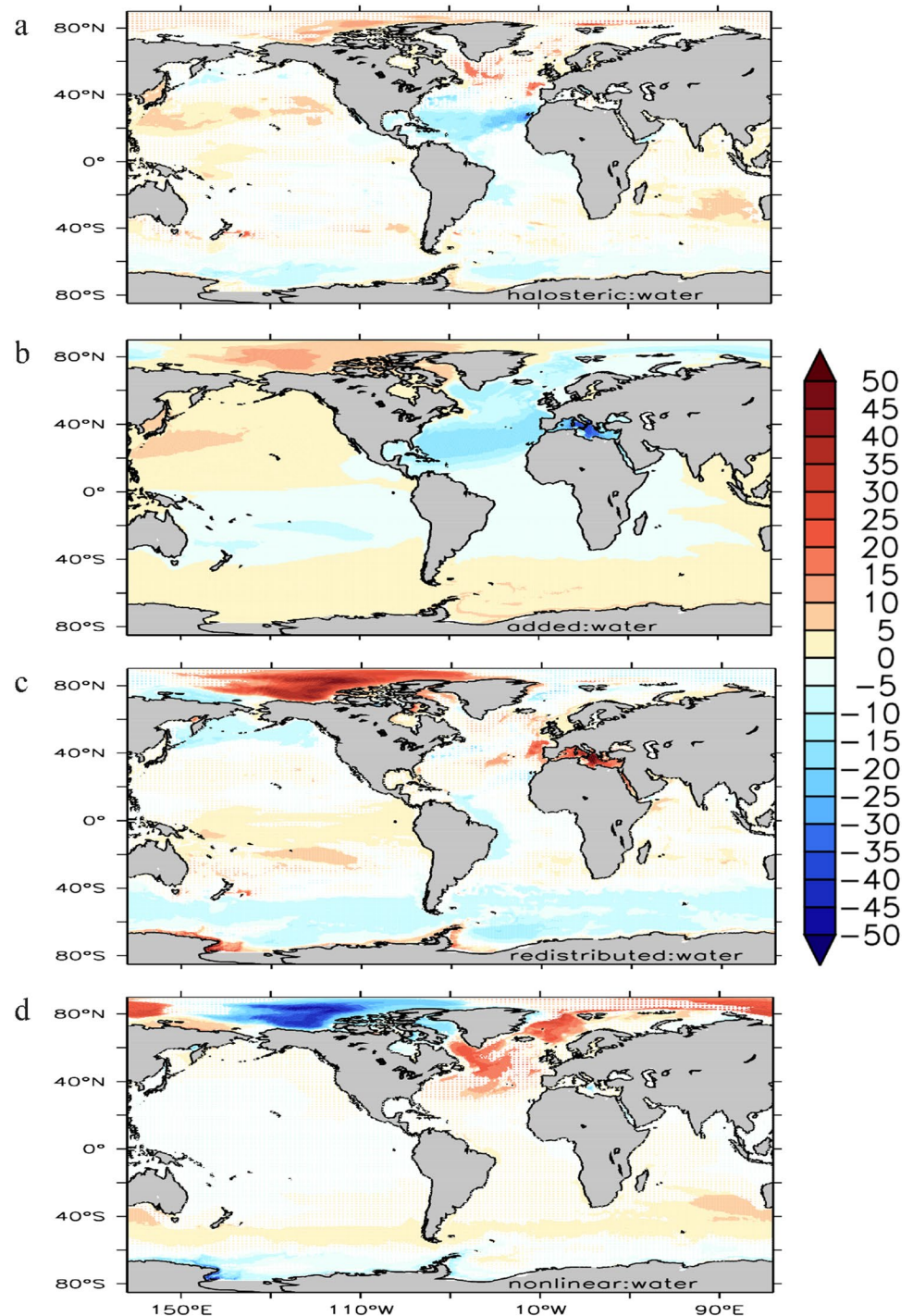
Freshening also appears to lower sea level in the Southern Ocean and south Pacific. Most of the other parts of the world ocean show a positive halosteric sea level rise.

A comparison with Fig. 7b, showing the sea level change resulting from the added water, confirms that most of the pattern of the halosteric seal level changes agree with local addition of freshwater. Nevertheless, the changes in the Arctic get even more enhanced through the redistribution

of freshwater (Fig. 7c), which is the leading cause for negative sea level changes over the Southern Ocean. Both together would create significantly larger halosteric sea level changes if there would not be nonlinear contributions that are as large as either of the others but mostly of opposite amplitude. Specifically the North Atlantic shows substantial positive nonlinear halosteric amplitudes, while for the Arctic the opposite holds. In both regions the existence of the

Fig. 8 Global zonal average of the thermosteric sea level of **a** FAF-heat (black line) and the contributions from added (red line), redistributed (green line) and the nonlinear term (blue line). **b** The contributions to redistributed thermosteric sea level from different experiments, i.e., the sum of FAF-stress, FAF-heat and FAF-water (black line), FAF-stress (red line), FAF-heat (green line) and FAF-water (blue line), respectively. Unit is in cm
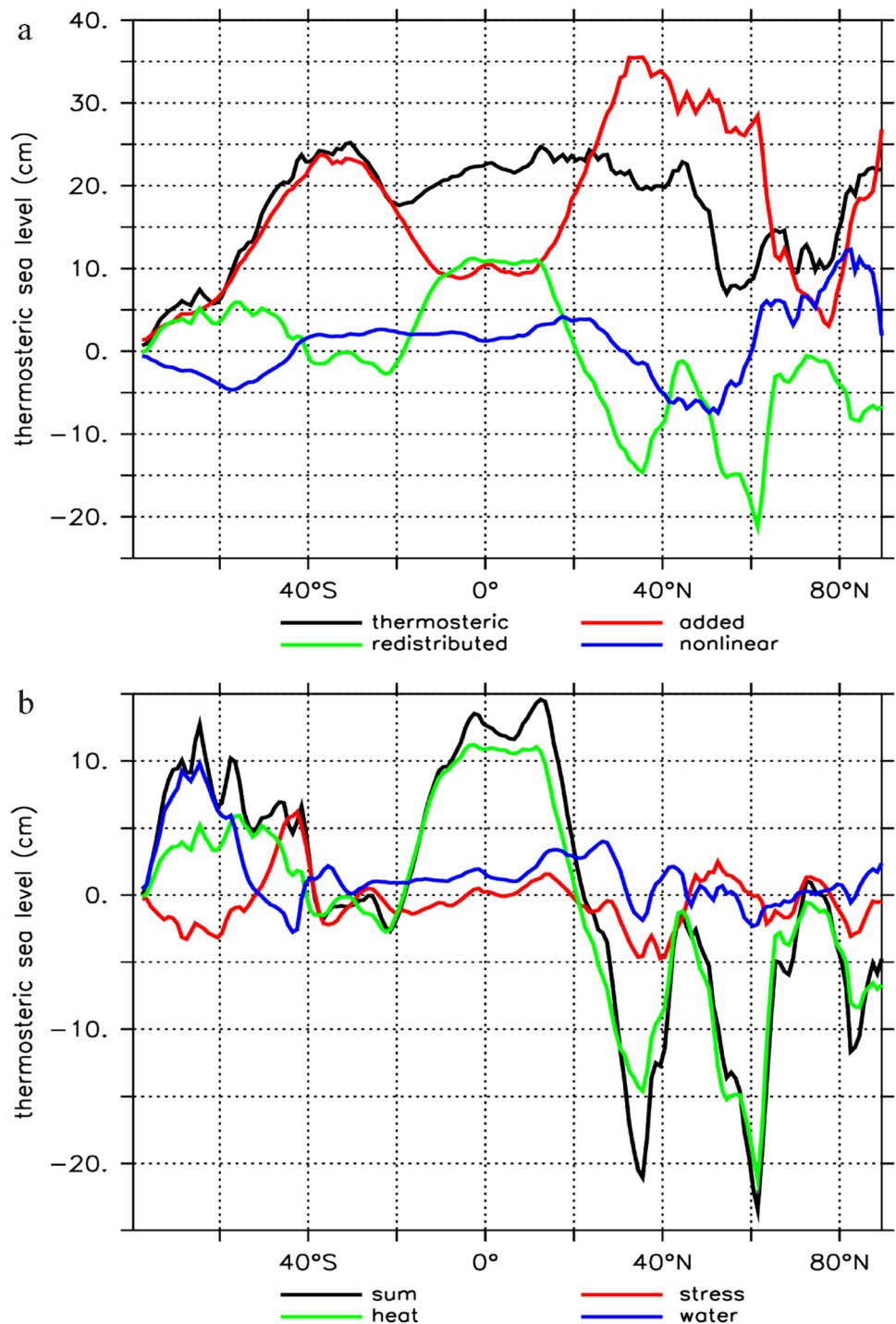

correlation between salt changes and current changes (v'S') is essential for shaping and actually reducing the resulting sea level change.

Global zonal averages of the total thermosteric and halosteric SL, as well as their redistributed, added and nonlinear components, are shown in Figs. 8 and 9, respectively. The only latitude range where thermosteric sea level seems to be dominated through local addition of heat appears to be

the southern hemisphere between 40 and 20 °S. Between 20 °S and 20 °N, the total thermosteric sea level increase is made up largely by the local addition and the redistribution of heat. North of 20 °N, the local addition of heat is partly counterbalanced by a negative redistribution of heat. Nonlinear contributions are significant outside tropical latitudes and up to 40 °S leading to negative contributions over the Southern Ocean and especially at the latitude of the North

**Fig. 9** As in Fig. 8, but for zonal mean of halosteric sea level
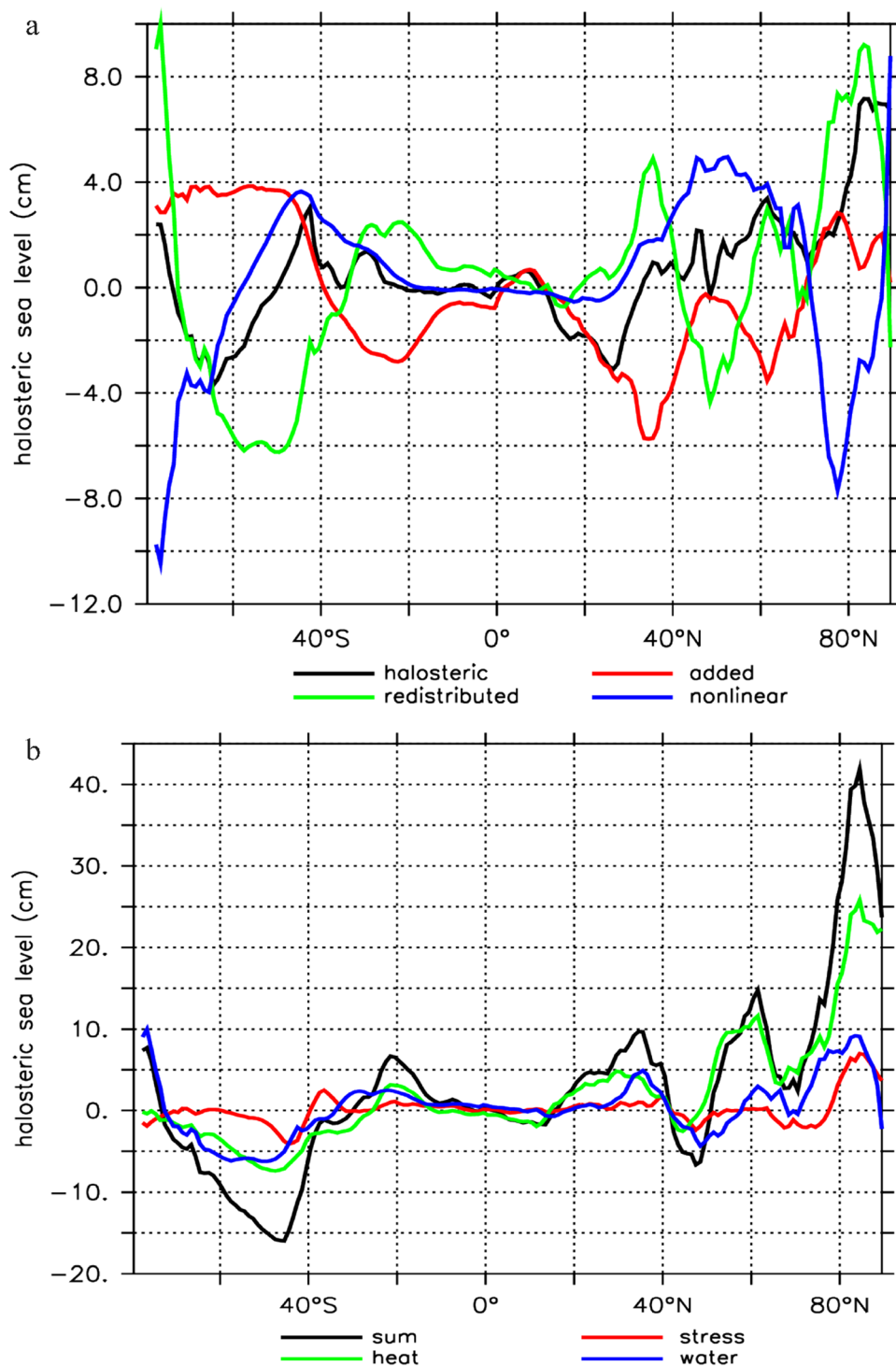
Atlantic Current. Nonlinear contributions are especially large over the Arctic where they are of the same order of magnitude as the local addition.

With respect to the zonally averaged halosteric component (Fig. 9a), the total is made up by all three components which all show up with equal amplitudes. At most latitudes the added and redistributed components compensate each other, only

north of 50 °N they are in phase. For the in-phase case, the non-linear component is mostly out of phase with the other two; for the compensation, it is in phase with the added component, e.g., in the Southern Ocean where the redistributed component then compensates a part of the other two. Obvious from the figure is also that over the Arctic the contribution from the nonlinear component results in only a 50% halosteric

Fig. 10 Redistributed thermosteric sea level and its components from different experiments **a** the sum of FAF-stress, FAF-heat and FAF-water, **b** FAF-stress, **c** FAF-heat and **d** FAF-water. Units are cm. Regions outside the white stippled areas are significant at the 95% level
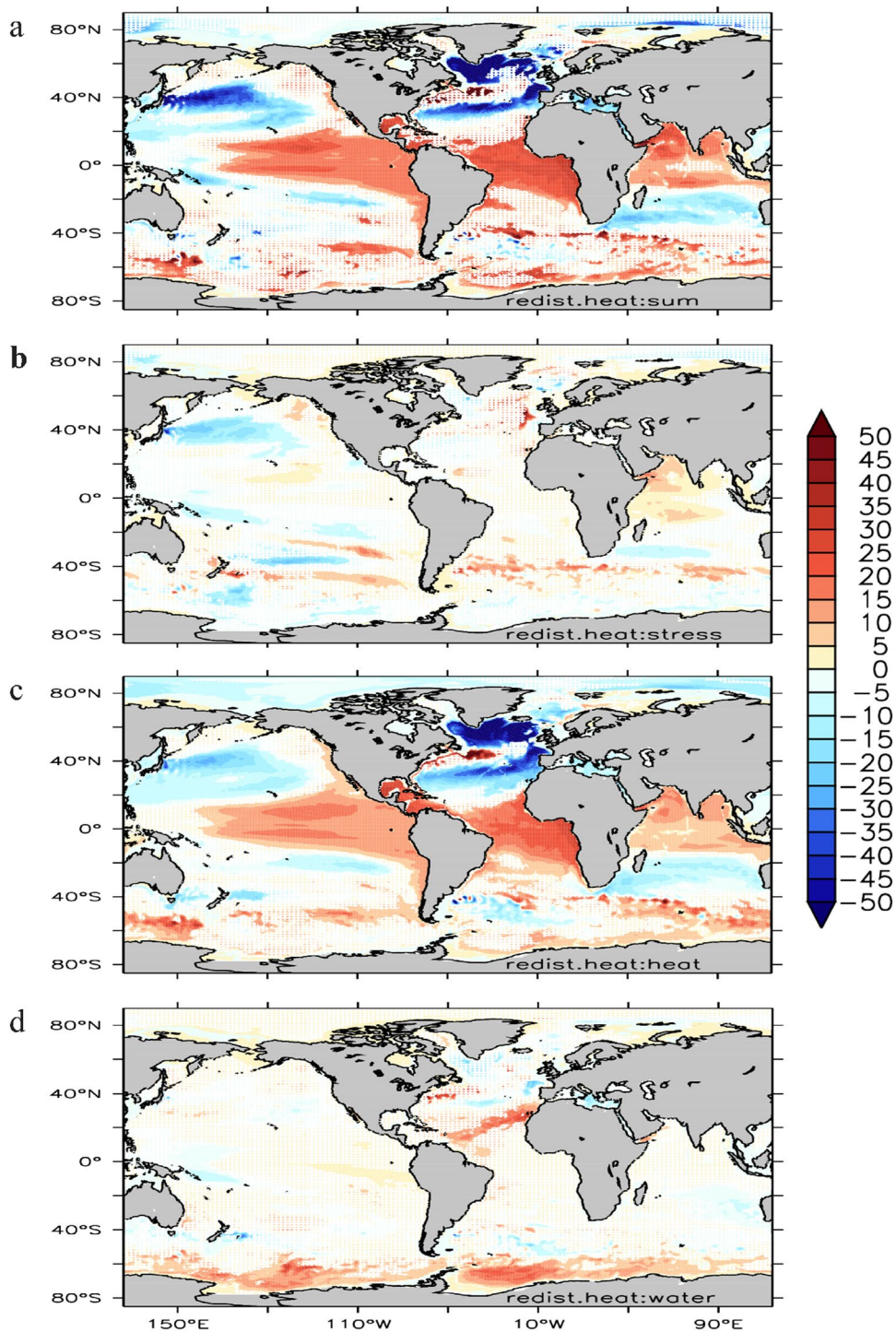
sea level increase that would not exist otherwise. The same holds between 40 and 60 °N, but with opposite sign, i.e., the halosteric sea level decline is only 50% of what it would be without the nonlinear contribution. Between the equator and 40°N the non-linear component and the halosteric sea level rise disappear, meaning the added and redistributed components balance.

4 Mechanisms

4.1 Redistributing heat and freshwater

To quantify the impact of redistribution on sea level response to all FAFMIP forcing we show in Fig. 10 the thermosteric redistribution of sea level as it results individually from FAF-stress (Fig. 10b), FAF-heat (Fig. 10c)

and FAF-water (Fig. 10d), as well as the sum of all of them (Fig. 10a). Clearly the heat flux perturbation shows the largest redistribution effect. However, this response is compensated substantially by the wind and freshwater impact so that the net response on the FAF-all experiment is only 50% of what it would be in the pure heat forcing experiment (compare Fig. 5). This holds especially for the North Atlantic, where also the heat impact is largest. But a reduction in the net response relative to the pure heating response is visible in all other basins. We note that—against expectations—the FAF-stress experiment has the smallest redistribution and that most of the compensation of the pure heating response actually comes from the freshwater forcing, implying that we always have to consider the net sea level response to be a superposition of both (heat and freshwater forcing) and not just a result of heating.

Zonal averages of the SL fields shown in Fig. 8 highlight the strong role that the heat flux perturbation plays in setting the redistributed thermosteric sea level change (Fig. 8b). The figure also highlights that on zonal average, the stress contribution acts in reducing the response that the heating alone would lead to; sometimes this is in phase with the freshwater contribution (north of 40 °N), sometimes it is out of phase (south of 40 °S).

Different from our result, Couldrey et al. (2021) show that the wind stress also plays an important role in opposing the heat-related SL pattern in the subtropical Pacific Ocean (around 45°) (see their Figs. 7c, 8c, 10c). They also conclude that in the North Atlantic Ocean, both heat flux and freshwater flux forcing are important and contribute to the dipole pattern. In contrast, in the Southern Ocean, the wind forcing is the dominant pattern (positive along 30–60 °S band and negative southward, as suggested by Gregory et al. 2016). Freshwater forcing plays the opposite role south of 60 °S, whereas heating enhances the positive pattern along 30–60 °S band and reduces the negative pattern south of 60 °S (see Fig. 6a–c in Couldrey et al. 2021).

Turning to the redistributed halosteric response (Fig. 11), we find again the largest response resulting from the heating experiment. However, now this response is not compensated by the others but in many places enhanced. The latter holds especially over the Arctic and over most of the northern hemisphere. But the Southern Ocean also shows a much stronger—negative—response in the superposition than present in any of the individual contributions. In addition, the sum of all contributions shows a more complex spatial structure than individual responses would suggest.

The relatively small impact of wind stress on the redistributed halosteric sea level is also obvious in the zonal averages shown in Fig. 9b. This holds especially in the southern hemisphere; only north of 40 °N a significant wind contribution can be seen that is comparable with the freshwater

forcing experiment. Interestingly, the heating and freshwater forcing push sea level in a similar direction over most regions. Only in the band 48–75 °N the components are out of phase and compensate each other partially so that the net response is smaller and the heating would cause alone.

4.2 Feedbacks in surface forcing fields

From the above discussion, it is obvious that all individual forcing terms project on all sea-level change components. It is also obvious and against expectations—that the heat flux perturbation experiment projects strongly on halosteric sea level anomalies, including their redistributed component. To understand why this is the case we analyze in the following the net surface forcing anomalies as they act in the coupled model. Since the coupled system has the freedom to react to any perturbation in the system it has to be expected that these net forcing anomalies differ from the FAFMIP imposed forcing anomalies (e.g., see Fig. 1 in Couldrey et al. 2021).

Shown in Fig. 12 are fields of the net surface heat flux as they follow from the experiments, FAF-all (Fig. 12a), the sum of the individual experiments (Fig. 12b), as well as for FAF-stress (Fig. 12c), FAF-heat (Fig. 12d), and FAF-water (Fig. 12e), respectively. Similar fields, but for the freshwater forcing and the wind stress forcing are shown in the same order in Figs. 13 and 14, respectively. For all forcing fields we see that the FAF-all experiment shows roughly the same net forcing that results from the sum of the individual experiments. Moreover, predominantly the resulting forcing appears to be largest for the heat flux forcing experiment, regardless of the stress, heat flux or freshwater flux fields. For the heat flux anomalies this is what we would expect because it includes the imposed forcing anomaly. However, looking at the freshwater analyzes (Fig. 13), we find the freshwater flux anomaly of the heat-flux experiment to be roughly double that of the FAF-water perturbation itself, with even larger signals particularly in the tropical Atlantic. A similar result can be found for the stress anomaly, which, northward of the Southern Ocean, is as large in the heat flux experiment as it would result from the FAF-stress anomaly.

In essence we find that applying a single forcing anomaly in a coupled system results in feedbacks in all other forcing fields that can be significant and that we always have to consider. Moreover, the feedbacks are associated with teleconnections and can communicate anomalies quickly around the globe through atmospheric pathways. The latter holds especially for wind stress anomalies (see also the discussion by Agarwal et al. 2014).

Fig. 11 As in Fig. 10, but for redistributed halosteric sea level and its contributions (unit: cm)
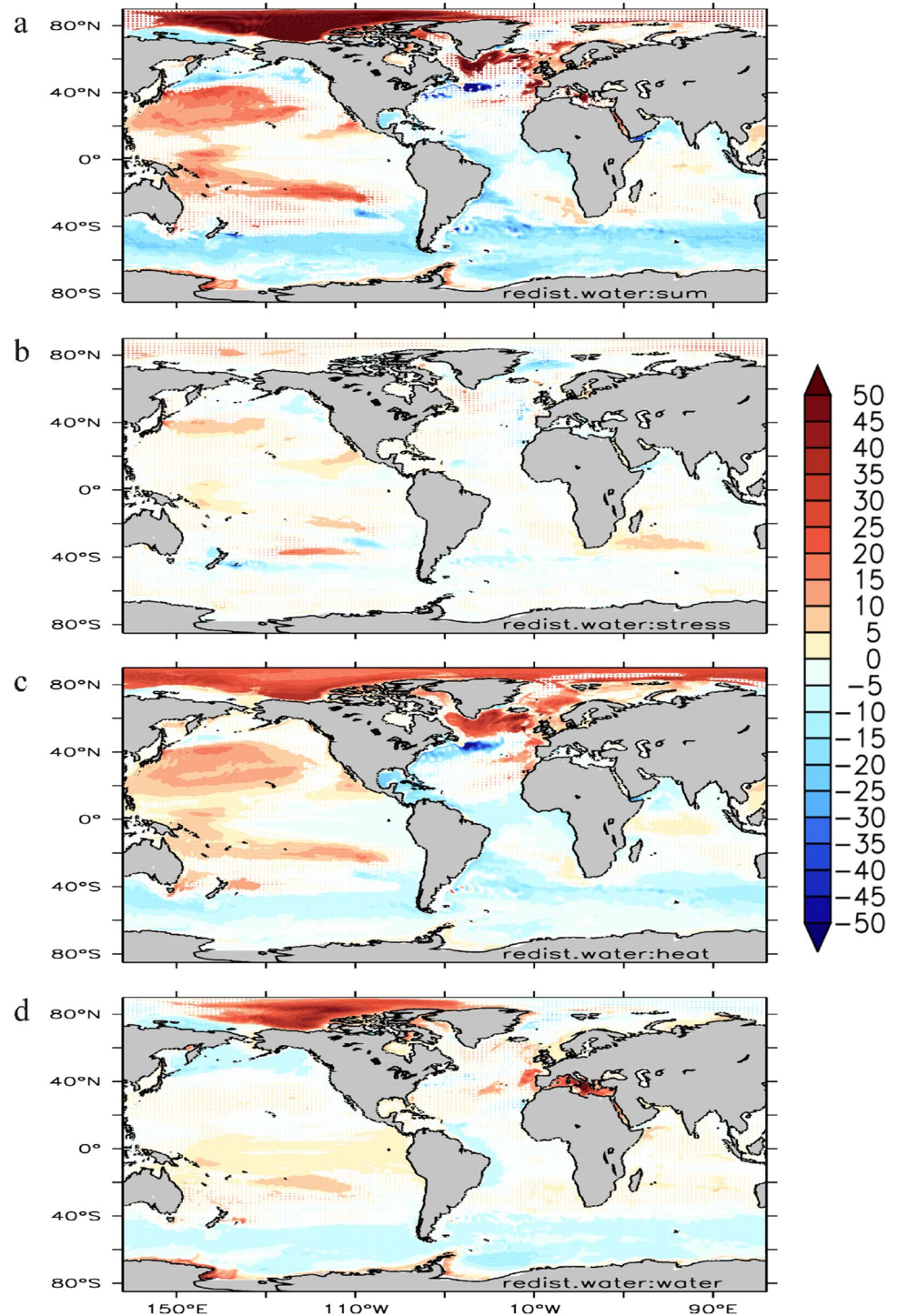
4.3 The role of surface stress anomalies

Köhl and Stammer (2008) and Frankcombe et al. (2013) demonstrated that for interannual variability the sea level is highly correlated with the barotropic stream function. But how large is the impact of changes in the gyre circulation on the SL resulting under FAFMIP conditions from the wind stress changes in each experiment? To answer this question,

we show in Fig. 15 the barotropic stream function based on different experiments and compare it with the pure Sverdrup response (Fig. 16) as it would result from just the wind stress anomalies in each experiment.

As before, the barotropic stream function as it results from FAF-all, roughly agrees with the sum of the contributions from the individual runs. However, the agreement is not quite as good as it appeared for individual forcing

Fig. 12 Heat flux (unit: W/m^2). **a** Total from FAF-all, **b** sum of FAF-stress, FAF-heat, and FAF-water, **c** FAF-stress, **d** FAF-heat, **e** FAF-water. Regions outside the white stippled areas are significant at the 95% level
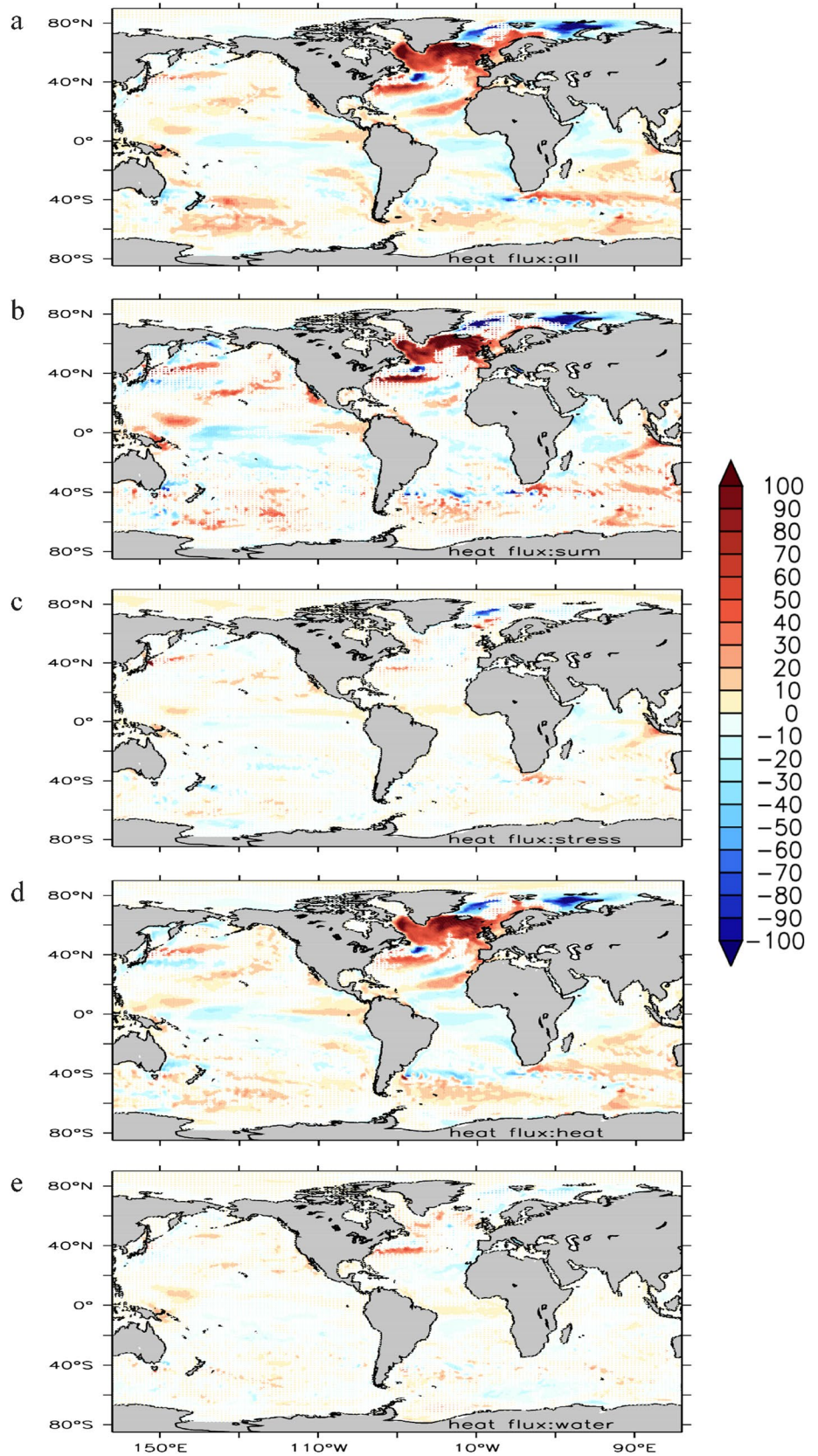
Fig. 13 As in Fig. 12, but for fresh water flux (unit: mm/year)
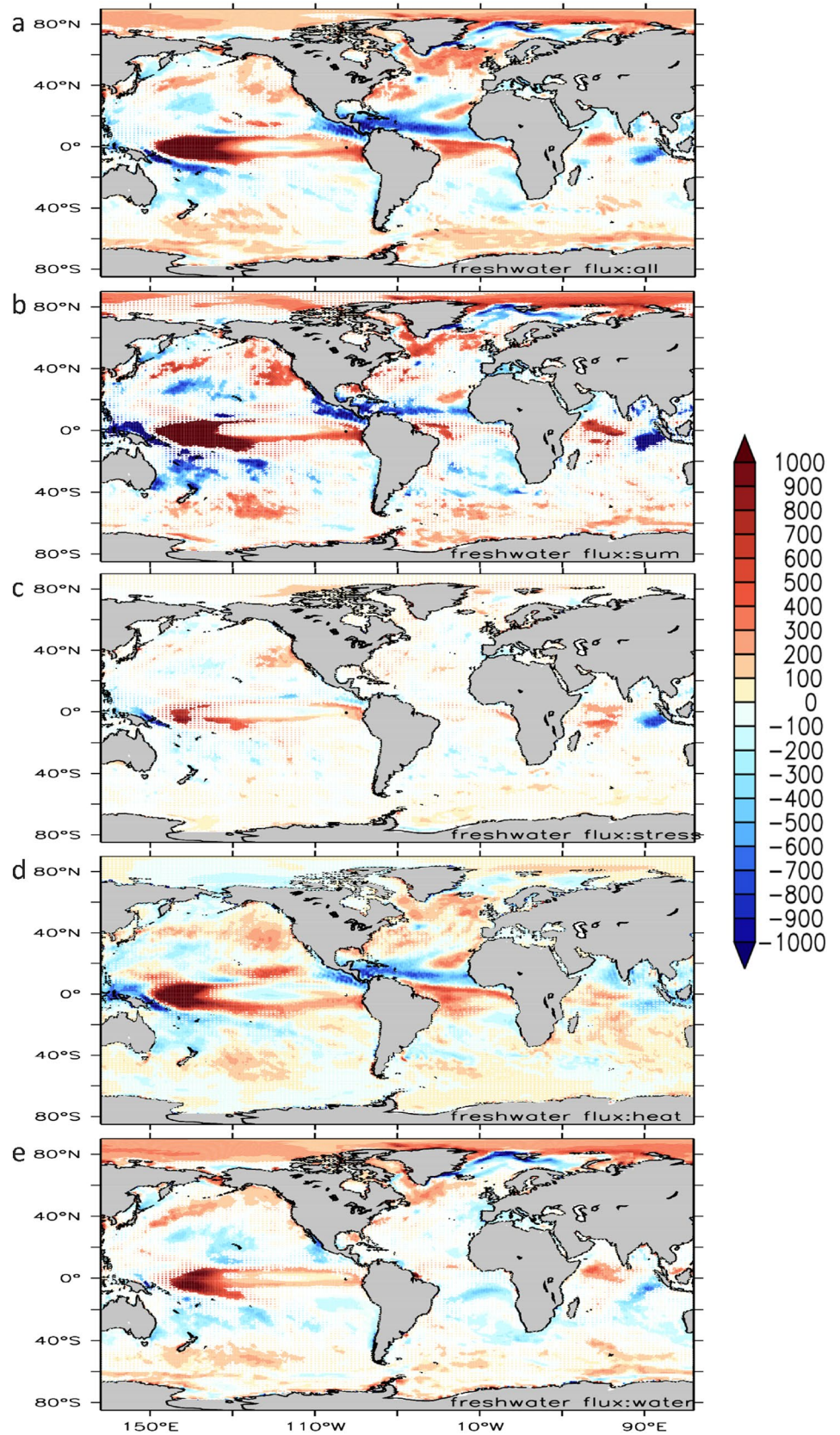
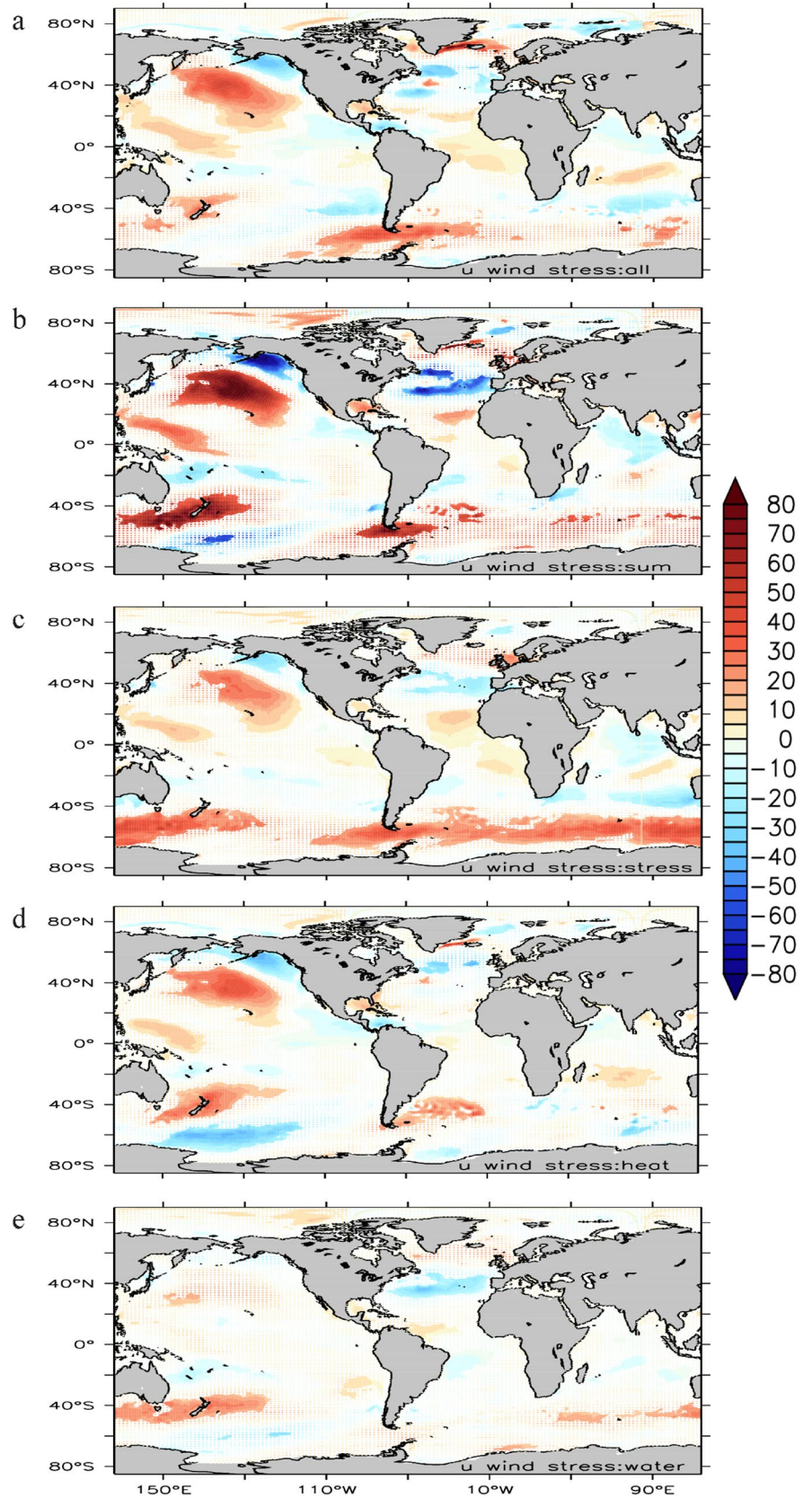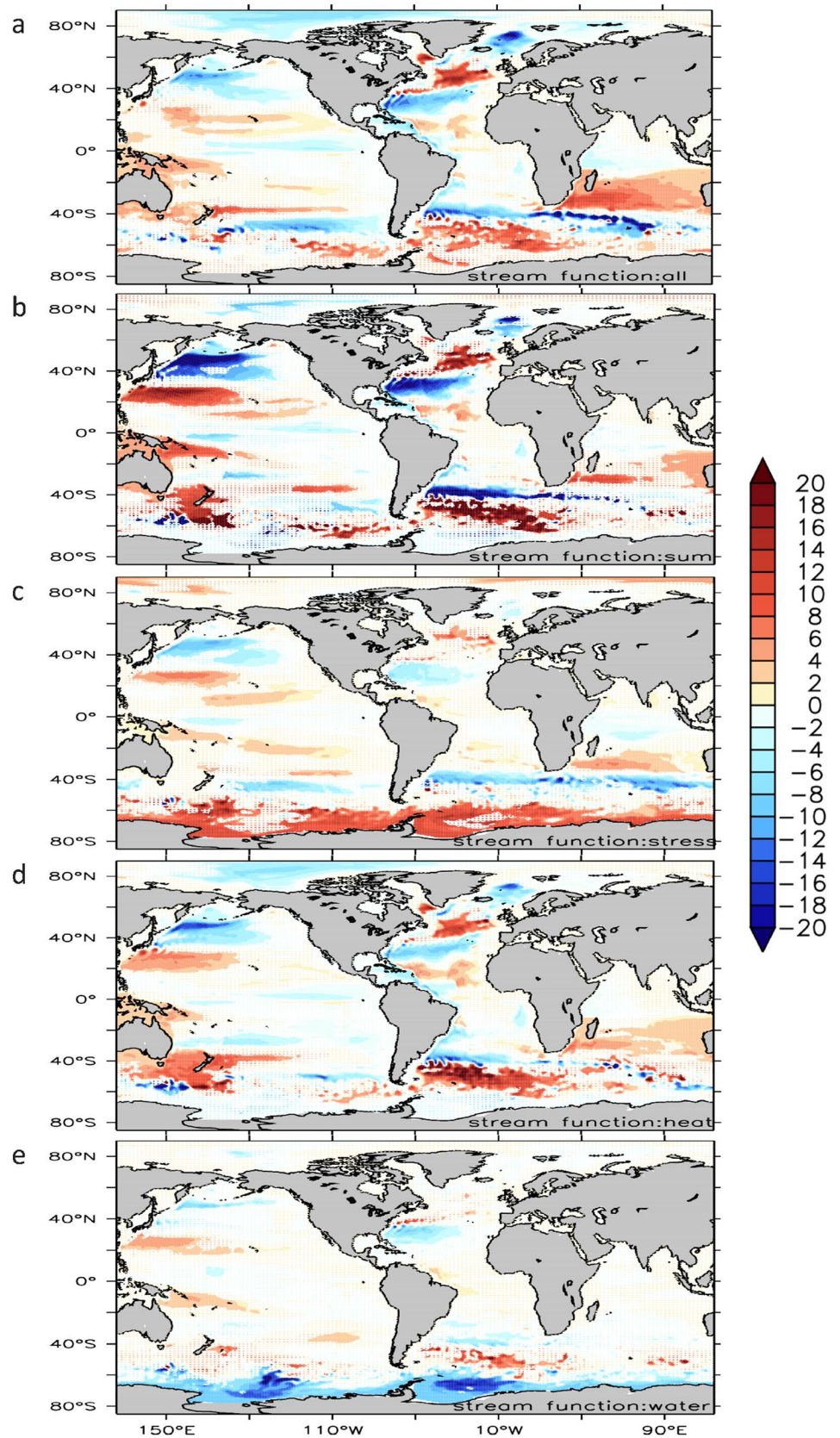**Fig. 14** As in Fig. 12, but for zonal wind stress (unit: mN/m²)

Fig. 15 Barotropic stream functions (Unit: Sv) as **a** total from FAF-all, **b** sum = FAF-stress + FAF-heat + FAF-water, **c** FAF-stress, **d** FAF-heat, **e** FAF-water. Regions outside the white stippled areas are significant at the 95% level

Fig. 16 Sverdrup stream functions (unit: Sv) from the zonal wind stress as **a** the total from FAF-all, **b** sum of FAF-stress, FAF-heat, and FAF-water, **c** FAF-stress, **d** FAF-heat, **e** FAF-water. Regions outside the white stippled areas are significant at the 95% level. Note the reduced range of the colorbar in comparison to Fig. 15
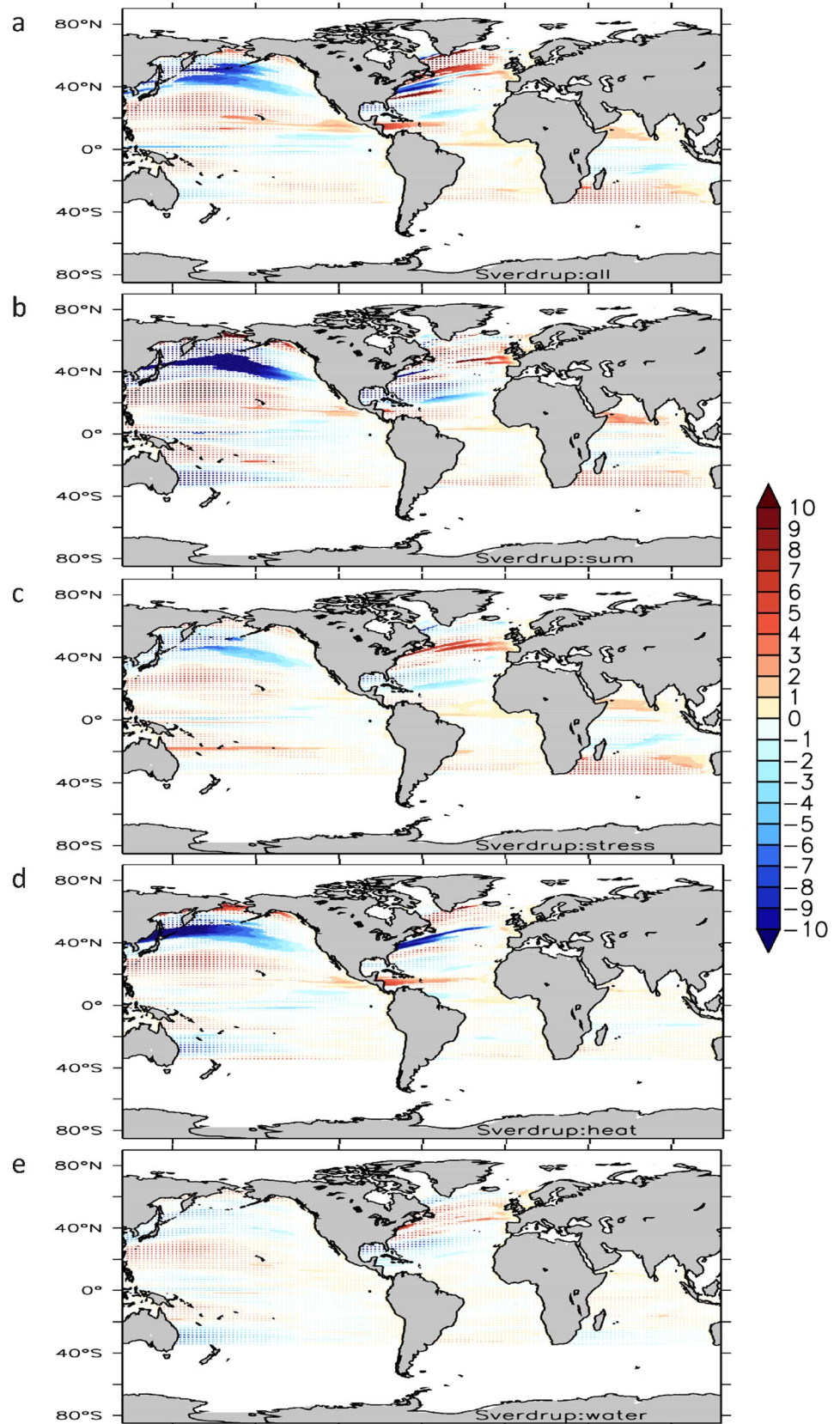
Table 2 Pattern correlation between the barotropic streamfunction and the Sverdrup streamfunction calculated over regions where the Sverdrup streamfunction is defined in Fig. 16 including regions of non-significant changes

Experiment	Pacific Ocean	Atlantic Ocean	Indian Ocean
FAF-all	0.60	0.12	0.73
FAF-stress	0.66	0.49	0.82
FAF-heat	0.64	0.00	0.48
FAF-water	0.66	0.38	− 0.41

components (Figs. 12, 13, 14). Differences are especially clear over the Southern Ocean, but also over parts of the subtropical and subpolar northern hemisphere, i.e., mostly dynamics regions in which the Sverdrup balance is not a useful approximation because of the importance of the topographic influence. We also note that the stream function anomaly is largest in the heat flux experiment, not in the wind stress experiment, especially in the northern hemisphere where according to Yeager (2015) overturning and gyre circulation are coupled through the bottom torque term.

How much of the stream function anomalies can be explained by the wind-driven Sverdrup response? A comparison of Figs. 15 and 16 (see also Table 2 for the pattern correlations calculated over the three ocean basins) reveals that in the Pacific Ocean and except for FAF-water also in the Indian Ocean much of the stream function anomalies of each experiment agree with the changes in the Sverdrup circulation. The Atlantic Ocean shows the lowest agreement reaching even for FAF-stress only a pattern correlation of 0.49. The implication of this is that outside of the Atlantic in each experiment it is the changes in the wind stress that is the primary cause for changes in the circulation and the resulting movement of the isopycnals cause the sea level response and the associated thermosteric or halosteric sea level changes. One has to note that the Sverdrup response is non-significant in much of the regions (nearly all for FAF-water), indicating the important influence of climate variability on the resulting wind stress anomalies. In particular, since all responses share the same state of the climate realized by the control, all responses share the common wind stress anomaly of the control run. The similarity between the Sverdrup responses (Fig. 16c–e) is obvious in the North Pacific but impacts other regions far less.

Looking at the southern hemisphere, the changes in the barotropic stream function are complex and are different between the individual experiments. Notably, the freshwater experiment leads here to significant negative anomalies not present in any of the other experiments. The origin of this signal is unclear, particularly since the wind stress changes are small in the Southern Ocean. However, the relation between wind stress changes and changes in barotropic stream function may not be as immediate

as assumed when calculating stream function responses based on the Sverdrup relation. Although in midlatitudes, circulation responses are fast and described by a time-depended Sverdrup balance (Willebrand et al. 1980), this does not hold for the Antarctic Circumpolar Current (ACC) (Olbers et al. 2004). Time-lags are variable but small for the barotropic component (Gille et al. 2001) and lags of 2–3 years between wind and circulation response were reported for the baroclinic component (Meredith and Hogg 2006; Yang et al. 2008). In fact, the decade before shows a zonal wind stress reduction of up to 30 N/m^2, such that the negative stream function signal could still be part of climate variability.

In conclusion, the difference in the spatial pattern of SL in the FAF-heat and FAF-stress experiments can largely be explained by the difference in the wind stress pattern. The wind stress is stronger in both the FAF-stress and FAF-water experiments resulting in an increase in SL whereas in FAF-heat a strong SL fall is visible in the same region. Apart from that, the North Pacific also shows a very strong wind stress response in most of the cases, which can be a reason for the SL change there. From the zonal mean it is clearly that wind stress anomalies resulting in FAF-heat through feedbacks are as large as those applied actively as perturbations in FAF-stress.

5 Discussion and concluding remarks

In this paper, we analyzed CMIP6 FAFMIP sea level anomaly patterns with respect to mechanistic causes as they emerge after imposing individual CMIP5-derived forcing anomalies in wind stress, heatflux and freshwater flux to the MPI-M model. Overall, we find similar patterns in the sea level response to the all-forcing perturbations compared to those in the 1pctCO2 experiment; however, amplitudes are about twice as large. Our results confirm previous conclusions (e.g., Gregory et al. 2016; Couldrey et al. 2021) that the heat flux perturbation leads to the largest impact on SL response and that the largest impact of surface flux perturbations on sea level is thermosteric in nature. However, we show here that because of feedback processes between individual forcing components existing in the coupled system, at the end it is always a superposition of all forcing components that together are responsible for the simulated sea level changes in each individual experiment and that one cannot pint-point the response to one seeming single cause. Instead, we demonstrate that through the respective feedback mechanisms it is actually the wind stress resulting from the other flux perturbations appears as the primary driving agent for changes of sea level outside of the Atlantic in all three experiments. Respective anomalies appear to be strongest in the heat flux anomaly experiment instead of the wind

stress anomaly experiment because the positive feedback in the North Atlantic almost doubles the heat flux perturbation there. The associated wind driven Sverdrup stream function implicates that outside of the Atlantic most of the feedback can be explained by changes in the wind driven Sverdrup circulation. However, Sverdrup responses are largely non-significant, demonstrating the important influence of climate variability in particular for the North Pacific, where all experiments share the same response patterns.

A detailed analysis of thermosteric and halosteric SL changes reveals that the thermosteric dominates the total SL and halosteric component mainly contributes north of 60 °N. The estimation of the added and redistributed components further suggest that the added component dominates the thermosteric SL and the redistributed component dominates the halosteric SL. The strong impact of heat flux in causing the SL change outside of the Southern Ocean and north of 60 ºN is evident whereas the freshwater flux is mostly counter acting poleward of 40 °N/S except some parts of the Arctic Ocean.

It remains to be shown to what extent results discussed here are generally robust or specific to the detailed model and model set up. It needs to be investigated to what extent small-scale processes not properly represented in the underlying MPI-ESM model could offset analyzed changes and underlying mechanisms. In the atmosphere and the ocean components of the model these could be eddy and weather processes that in principle could offset some of the large-scale changes. Respective work is beyond the scope of this paper and will be shown elsewhere.

Declarations

Conflict of interest The authors declare that they have no conflict of interest.

References

Agarwal N, Köhl A, Mechoso R, Stammer D (2014) On the transient impact on the climate system of a meltwater input from Greenland. J Clim 27:8276–8296. https://doi.org/10.1175/JCLI-D-13-00762.1

Carson M, Köhl A, Stammer D (2015) The impact of regional multi-decadal and century-scale internal climate variability on sea level trends in CMIP5 models. J Clim 28(2):853–861. https://doi.org/10.1175/JCLI-D-14-00359.1

Carson M, Köhl A, Stammer D et al (2016) Coastal sea level changes, observed and projected during the 20th and 21st century. Clim Change 134(1–2):269–281. https://doi.org/10.1007/s10584-015-1520-1

Couldrey MP, Gregory JM, Diasaffil FB et al (2021) What causes the spread of model projections of ocean dynamic sea level change in response to greenhouse gas forcing? Clim Dyn 56:155–187. https://doi.org/10.1007/s00382-020-05471-4

Garuba OA, Klinger BA (2016) Ocean heat uptake and interbasin transport of the passive and redistributive components of surface heating. J Clim 29(20):7507–7527

Gill AE, Niiler PP (1973) The theory of the seasonal variability in the ocean. Deep-Sea Res 20:141–177. https://doi.org/10.1016/0011-7471(73)90049-1

Gille ST, Stevens DP, Tokmakian RT, Heywood KJ (2001) Antarctic Circumpolar Current response to zonally averaged winds. J Geophys Res 106(C2):2743–2759. https://doi.org/10.1029/1999JC900333

Gregory J, Bouttes-Mauhourat N, Griffies SM et al (2016) The Flux-Anomaly-Forced Model Intercomparison Project (FAFMIP) contribution to CMIP6: investigation of sea-level and ocean climate change in response to CO_2 forcing. Geosci Model Dev. https://doi.org/10.5194/gmd-2016-122

Jungclaus JH, Fischer N, Haak H, Lohmann K, Marotzke J, Matei D, Mikolajewicz U, Notz D, von Storch JS (2013) Characteristics of the ocean simulations in the Max Planck Institute Ocean Model (MPIOM) the ocean component of the MPI-Earth System Model. J Adv Model Earth Syst 5(2):422–446. https://doi.org/10.1002/jame.20023

Landerer FW, Jungclaus JH, Marotzke J (2007) Regional dynamic and steric sea level change in response to the IPCC-A1B scenario. J Phys Oceanogr 37(2):296–312. https://doi.org/10.1175/JPO3013.1

Mauritsen T, Bader J, Becker T et al (2019) Developments in the MPI-M Earth System Model version 1.2 (MPI-ESM1.2) and its response to increasing CO_2. J Adv Model Earth Syst 11(4):998–1038. https://doi.org/10.1029/2018MS001400

Meredith MP, Hogg AM (2006) Circumpolar response of Southern Ocean eddy activity to a change in the Southern Annular Mode. Geophys Res Lett 33:L16608. https://doi.org/10.1029/2006GL026499

Müller WA, Jungclaus JH, Mauritsen T et al (2018) A high-resolution version of the Max Planck Institute Earth System Model

MPI-ESM1.2-HR. J Adv Model Earth Syst 10:1383–1413. https://doi.org/10.1029/2017MS001217

Olbers D, Borowski DANIEL, Völker C, Wolff JO (2004) The dynamical balance, transport and circulation of the Antarctic Circumpolar Current. Antarct Sci 16(4):439–470. https://doi.org/10.1017/S0954102004002251

Pardaens AK, Gregory JM, Lowe JA (2011) A model study of factors influencing projected changes in regional sea level over the twenty-first century. Clim Dyn 36(9–10):2015–2033. https://doi.org/10.1007/s00382-009-0738-x

Slangen ABA, Carson M, Katsman CA, van de Wal RSW, Köhl A, Stammer D (2014) Projecting twenty-first century regional sea-level changes. Clim Change 124:317–332. https://doi.org/10.1007/s10584-014-1080-9

Stammer D, Cazenave A, Ponte RM, Tamisiea ME (2013) Contemporary regional sea level changes. Ann Rev Mar Sci 5:21–46. https://doi.org/10.1146/annurev-marine-121211-172406

Stevens B, Giorgetta M, Esch M et al (2013) Atmospheric component of the MPI-M earth system model: ECHAM6. J Adv Model Earth Syst 5(2):146–172. https://doi.org/10.1002/jame.20015

Todd A, Zanna L, Couldrey M et al (2020) Ocean-only FAFMIP: understanding regional patterns of ocean heat content and dynamic sea level change. J Adv Model Earth Syst. https://doi.org/10.1029/2019MS002027

Willebrand J, Philander SGH, Pacanowski RC (1980) The oceanic response to large-scale atmospheric disturbances. J Phys Oceanogr 10(3):411–429. https://doi.org/10.1175/1520-0485(1980)010

Yang X, Huang R, Wang J, Wang D (2008) Delayed baroclinic response of the Antarctic circumpolar current to surface wind stress. Sci China, Ser D Earth Sci 51(7):1036–1043. https://doi.org/10.1007/s11430-008-0074-8

Yeager S (2015) Topographic coupling of the Atlantic overturning and gyre circulations. J Phys Oceanogr 45(5):1258–1284. https://doi.org/10.1175/JPO-D-14-0100.1